THE JOURNAL OF BIOLOGICAL CHEMISTRY VOL. 288, NO. 40, pp. 29170–29181, October 4, 2013

Homotypic Versican G1 Domain Interactions Enhance Hyaluronan Incorporation into Fibrillin Microfibrils*

Received for publication, January 29, 2013, and in revised form, July 31, 2013 Published, JBC Papers in Press, August 20, 2013, DOI 10.1074/jbc.M113.456947

Yusuke Murasawa[‡], Ken Watanabe[§], Masahiko Yoneda[¶], Masahiro Zako[‖], Koji Kimata[**], Lynn Y. Sakai[‡‡], and Zenzo Isogai[‡1]

From the [‡]Department of Advanced Medicine and [§]Department of Bone and Joint Disease, National Center for Geriatrics and Gerontology, Obu, Aichi 474-8511, Japan, the [¶]School of Nursing and Health, Aichi Prefectural University, Nagoya, Aichi 463-8502, Japan, the [‖]Department of Ophthalmology and [**]Research Complex for Medical Frontiers, Aichi Medical University, Nagakute, Aichi 480-1195, Japan, and the [‡‡]Shriners Hospital for Children and Department of Biochemistry and Molecular Biology, Oregon Health and Science University, Portland, Oregon 97239

Background: Versican interacts with hyaluronan (HA) via its G1 domain and with fibrillin microfibrils via its G3 domain. However, the roles of versican G1 domain-containing fragments (VG1Fs) in the HA-versican-microfibril macrocomplex are not clear.
Results: VG1Fs interact homotypically and are recaptured by versican-containing fibrillin microfibrils.
Conclusion: Homotypical interactions of VG1Fs enhance HA recruitment to microfibrils.
Significance: VG1Fs stabilize HA-versican-microfibril macrocomplexes.

Versican G1 domain-containing fragments (VG1Fs) have been identified in extracts from the dermis in which hyaluronan (HA)-versican-fibrillin complexes are found. However, the molecular assembly of VG1Fs in the HA-versican-microfibril macrocomplex has not yet been elucidated. Here, we clarify the role of VG1Fs in the extracellular macrocomplex, specifically in mediating the recruitment of HA to microfibrils. Sequential extraction studies suggested that the VG1Fs were not associated with dermal elements through HA binding properties alone. Overlay analyses of dermal tissue sections using the recombinant versican G1 domain, rVN, showed that rVN deposited onto the elastic fiber network. In solid-phase binding assays, rVN bound to isolated nondegraded microfibrils. rVN specifically bound to authentic versican core protein produced by dermal fibroblasts. Furthermore, rVN bound to VG1Fs extracted from the dermis and to nondenatured versican but not to fibrillin-1. Homotypic binding of rVN was also seen. Consistent with these binding properties, macroaggregates containing VG1Fs were detected in high molecular weight fractions of sieved dermal extracts and visualized by electron microscopy, which revealed localization to microfibrils at the microscopic level. Importantly, exogenous rVN enhanced HA recruitment both to isolated microfibrils and to microfibrils in tissue sections in a dose-dependent manner. From these data, we propose that cleaved VG1Fs can be recaptured by microfibrils through VG1F homotypical interactions to enhance HA recruitment to microfibrils.

The connective tissue is composed of a network of extracellular matrix (ECM)[2] macromolecules. Proper coordination of the production, assembly, and degradation of ECM molecules is responsible for the physical properties of connective tissues, and fragmentation of the ECM by cleavage of intact molecules plays a dynamic role in connective tissue remodeling (1).

Versican is a large chondroitin sulfate proteoglycan that interacts with hyaluronan (HA) via its G1 domain at the amino terminal (2–4). Versican also binds to fibrillin-1, fibulin-1, and fibulin-2 via a G3 domain at the carboxyl terminal and is codistributed in a variety of connective tissues with fibrillin microfibrils (5–8). Therefore, intact versican bound to fibrillin connects the HA-rich matrix to the elastic fiber network.

Fibrillin microfibrils consist of fibrillins and ubiquitous connective tissue elements that exhibit a characteristic "beads and strings" morphology after extraction from tissues, rotary shadowing, and electron microscopy (9–11). The molecular organization and, presumably, the function of microfibrils differ between tissues, depending on the age of the tissue and on the predominant fibrillin subtype (11, 12). Because the localization of versican, as determined by light and electron microscopy, is not completely identical to that of fibrillin microfibrils, versican may impart tissue-specific functions to microfibrils (8, 13).

A loss of the G1 domain of versican can be observed in solar elastosis, where the interaction between HA and microfibrils is also lost in the dermis (14). Moreover, isolated microfibrils from the ciliary body and vitreous humour exhibit different morphologies and HA-binding abilities because of the presence of the G1 domain of versican (15). Therefore, the versican G1 domain may be a critical modulator of tissue-specific functions of fibrillin microfibrils through interactions with HA.

* This work was supported by grants-in-aid from the Ministry of Health, Labor, and Welfare of Japan (to Z. I., K. W., and M. Y.), by a grant from the Mizutani Foundation (to Z. I.), and by a grant from Shriners Hospital for Children (to L. Y. S.).

The amino acid sequence of this protein can be accessed through NCBI Protein Database under NCBI accession number NP_001157569.

[1] To whom correspondence should be addressed: 35 Gengo, Morioka-cho, Obu, Aichi 474-8511, Japan. Tel.: 81-562-46-2311 ext. 7156; Fax: 81-562-48-2373; E-mail: zenzo@ncgg.go.jp.

[2] The abbreviations used are: ECM, extracellular matrix; HA, hyaluronan; VG1F, versican G1 domain-containing fragment; ADAMTS, a disintegrin and metalloproteinases with thrombospondin motifs; pAb, polyclonal antibody; NHDF, normal human dermal fibroblast; HABP, hyaluronan-binding protein; bHA, biotin-conjugated hyaluronan.

Versican G1 domain-containing fragments (VG1Fs) are generated through cleavage of versican by ADAMTS-1, ADAMTS-4, ADAMTS-5, and ADAMTS-9 (16, 17). Versican is also susceptible to matrix metalloproteinases (18). Moreover, it has been reported that VG1Fs can be extracted from normal skin (14, 19, 20) and that the quantity of VG1Fs varies during skin development and aging (18, 19). VG1Fs are also found in other tissues, such as the brain and aorta (16, 21). Although VG1Fs exist in tissues as versican cleavage products, the functions of VG1Fs have not yet been elucidated.

In this study, we focus on the structural properties and function of VG1Fs. Our results indicate that VG1Fs can be incorporated into microfibrils through homotypical interactions. Furthermore, VG1Fs can enhance incorporation of HA into the microfibril matrix. Our findings highlight novel properties of VG1Fs and suggest an important role for VG1Fs in the formation of the microfibril-versican-HA complex.

EXPERIMENTAL PROCEDURES

Antibodies—Monoclonal 2B1 antibody, which recognizes human versican under nonreducing conditions (22), was purchased from Seikagaku Kogyo (Tokyo, Japan). Polyclonal antibodies for the G1 domain, pAb 6084 and pAb 7080, were characterized in our previous studies (14, 15), and pAb 8531 was raised against a synthetic peptide for the human versican neoepitope, NH_2-CGGDPEAAE-COOH, generated by ADAMTS proteases (16). Production of synthetic peptides and polyclonal antibodies were performed by Operon Biotechnology (Tokyo, Japan). Commercially available anti-DPEAAE antibody was purchased from Affinity Bioreagents (Golden, CO). Immunoreactivities with pAb 8531 and commercially available anti-DPEAAE antibodies were identical both in dermal extracts and in conditioned medium from dermal fibroblasts (data not shown). pAb 9543, specific for fibrillin-1 (23), was used. mAb 8A4, specific for link protein (24), and mAb 12C5, which recognizes the G1 domain of human versican, were obtained from the Developmental Studies Hybridoma Bank (Iowa University, IA). An mAb for elastin (clone BA-4) was purchased from Sigma. Recognition sites for anti-versican antibodies are shown in Fig. 1.

Cell Culture—Fetal normal human dermal fibroblasts (NHDFs, Lonza, Walkersville, MD) were maintained in DMEM supplemented with 10% fetal calf serum and penicillin-streptomycin in a 5% CO_2 atmosphere.

Expression of Recombinant Versican Polypeptides—Recombinant versican polypeptides containing globular domains were expressed as described previously (14). A polypeptide corresponding to the HA-binding region was expressed and characterized as rVN (14). For the construction of rVNβ, consisting of the G1 domain and the N-terminal portion of the chondroitin sulfate β domain, the region encoding Leu^{21} to Glu^{441} of human versican (V1) was amplified by PCR with the sense primer 5′-CCC GCT AGC ACA TCA TCA TCA TCA TCA TCT ACA TAA AGT CAA AGT GGG AAA AAG-3′, introducing an NheI restriction site and six histidine residues at the 5′ end, and the antisense primer 5′-GGC TCG AGT CAT TCT GCA GCT TCT GGG TCC TTG GG-3′ to generate a C-terminal region corresponding to the cleaved end after proteolysis by ADAMTS proteinases (Val^{433}PKDPEAAE). For the G3 domain of versican, rVC, the region encoding Gly^{3110} to Arg^{3485} of versican (V0) was amplified with the sense primer 5′-CCC GCT AGC ACA TCA TCA TCA TCA TCA TGG GCA GGA TTC CAC GAT AGC AG-3′, introducing an NheI restriction site and six histidine residues at the 5′ end, and the antisense primer 5′-GGG CTC GAG TCA GCG CCT CGA CTC CTG CCA CCT C-3′, introducing a sequence for a stop codon and an XhoI restriction site at the 3′ end. The NheI-XhoI fragments for VNβ or VC were subcloned into pCEP/γ2III4 containing the sequence for the BM40/SPARC (secreted protein acidic and rich in cysteine) signal peptide used to facilitate peptide secretion. All of the versican fragments amplified by PCR were confirmed by DNA sequencing. An episomal expression system using 293 EBNA cells was employed as described (25). The recombinant polypeptides were purified by chelating chromatography (Hi Trap chelating, GE Healthcare) and gel filtration under nondenaturing conditions as described previously (14). The expected sizes and N-terminal sequences of the polypeptides were confirmed by Edman degradation and Western blotting with anti-HRP-conjugated anti-His antibodies (Invitrogen). HA contamination was not detected in the preparation using biotin-conjugated HABP (Seikagaku Kogyo) (15). Fibrillin-1 recombinant polypeptides, rF11 and rF6, were also used. The production and characterization of these recombinant polypeptides has been described previously (8, 25).

Sequential Extraction of Dermis—Normal adult human dermis was extracted with three reagents, 6 M guanidine hydrochloride, 50 mM Tris-HCl, 1 mM PMSF, and 1% (v/v) protease inhibitor mixture (Sigma) (pH 7.5) (Gdn); PBS containing 1 mM PMSF and 1% (v/v) protease inhibitor mixture (PBS); and *Streptomyces* hyaluronidase (HAase). Hyaluronidase (100 TRU, Seikagaku Kogyo) treatment was performed in 50 mM acetate buffer at 37 °C for 6 h.

Pieces of normal-looking skin were obtained from individuals (70- and 74-year-old men) as excess tissue after skin surgery at various anatomical sites (buttocks and back) with written informed consent. This protocol was approved by the ethical committee of the National Center for Geriatrics and Gerontology. No pathological abnormalities were identified in the donor skin. Fat tissue was removed, and the trimmed dermal tissue was minced into ~1-mm pieces. Then, different extraction procedures were performed. In one experiment, dermal pieces (~200 mg) were initially extracted with 6 M Gdn solution at 4 °C for 72 h, and the supernatant was collected by centrifugation at 12,000 rpm for 10 min. The residual insoluble material was extracted with PBS at 4 °C for 24 h, and then the residue was treated with 100 TRU *Streptomyces* HAase. In another experiment, the extraction methods were modified as noted in Fig. 2.

Gel Filtration, Ultracentrifugation, and Rotary Shadowing Electron Microscopy—Extracts were sieved using Sepharose CL-2B (GE Healthcare) in 4 M guanidine hydrochloride and 50 mM Tris-HCl (pH 7.5) as described previously (26). In some experiments, the extract was concentrated with an Amicon concentrator (Amicon Ultra-4, 50-kDa cutoff, Millipore, MA) to reduce the volume and remove low molecular weight proteins. The total volume of the column was 320 ml. The high molecular weight void volume fractions were further separated

by ultracentrifugation and were brought to a density of 1.27 g/ml by the addition of cesium chloride (15). A gradient was created by centrifugation at 40,000 rpm for 48 h at 10 °C. Aggregates that reacted positively with pAb 6084 were fractionated at a density of 1.28 g/ml. The fractions were then dialyzed against water and visualized by electron microscopy after rotary shadowing (Hanaichi Electron Microscopy, Okazaki, Japan). The positive material (10 μg) was also treated with 0.01 mg/ml trypsin (proteomics grade, T6567, Sigma) in 1 ml of digestion buffer (50 mM NH_4HCO_3 (pH 8.5) with 5% acetonitrile) at 37 °C for 12 h. Some samples were further digested with 0.1 μg of V8 protease (Sigma) in 400 μl of 75 mM ammonium acetate (pH 4.0) containing 4 mM EDTA at 37 °C for 12 h. The digested samples were subjected to SDS-PAGE followed by staining with Coomassie Brilliant Blue or by immunoblotting with pAb 6084.

Western Blot Analysis and Blot Overlay Assay—Serum-free conditioned medium was obtained from NHDFs cultured for 72 h. Matrix extracts were prepared by the protocol for tissue described above. Some samples were treated with chondroitinase ABC for 30 min at 37 °C as described previously (22). Samples were resolved on 7.5% gels by SDS-PAGE unless indicated otherwise. For reducing conditions, dithiothreitol was added at a final concentration of 50 mM. Separated proteins were transferred onto nitrocellulose membranes. For washing and incubating, TBS containing 0.1% Tween 20 (TBST) was used. The membrane was blocked with 5% nonfat skim milk (Dako, Denmark) in TBST at room temperature for 1 h, followed by incubation with pAb 6084 (5 μg/ml), mAb 2B1 (1 μg/ml), or pAb 8531 (1:1000) in TBST containing 2% milk. HRP-conjugated anti-rabbit IgG or HRP-conjugated anti-mouse IgG (Dako) was used for detection, and development of the blots was facilitated by ECL (GE Healthcare).

A blot overlay assay was performed as described previously (27). After blocking with 5% milk in TBST for 1 h, the membrane was incubated with rVN (5 μg/ml) in 2% milk in TBS at room temperature for 3 h. For some experiments, biotin-conjugated rVN was prepared using a biotin labeling kit (Dojinbo, Kumamoto, Japan), according to the protocol of the manufacturer. To detect hyaluronan, biotin-conjugated HABP was used as described (15). The bound ligands were detected with HRP-conjugated anti-His antibodies (Invitrogen) or streptavidin-HRP (Invitrogen) incubated in 2% milk/TBST for 1 h and subsequently visualized by ECL.

Solid-phase Binding Assay—Microfibrils from human fetal membranes were isolated using guanidine extraction, gel filtration, and isopycnic ultracentrifugation containing cesium chloride, a procedure that has been used previously to purify nondegraded microfibrils (26). Fetal membranes were separated from a fully developed human placenta that had no pathological abnormalities. Isolated microfibrils (2.5 μg/ml, 200 μl) or recombinant polypeptides (2.5 μg/ml, 200 μl) were immobilized on multiwell plates (Sumilon, Tokyo, Japan) in carbonate buffer (pH 8.8) at 4 °C for 12 h and blocked with 5% nonfat skim milk in TBST at room temperature for 1 h as described previously (27). For some experiments using avidin detection, 0.1% BSA was used for blocking. The microfibril preparation reacted positively with pAb 6084 and mAb 2B1 by dot blotting, indicating that the G1 and G3 domains were present (data not shown). However, no contamination of HA was detected by biotin-conjugated HABP. Soluble ligands were serially diluted 3-fold in TBS containing 2 mM $CaCl_2$ and 0.1% BSA, beginning with an initial dilution to 10 μg/ml. For a negative control, reduced and alkylated rVN (indicated as rVN(r)) was generated as described (28). Soluble ligand, rVN, was incubated in the wells for 3 h at room temperature, and the bound rVN was detected after 2-h incubation with HRP-conjugated anti-His antibodies (Invitrogen) diluted 1:1000 (v/v) in 2% milk/TBST. To examine versican-versican interactions, rVN (5 μg/ml, 100 μl/well) or rVC (5 μg/ml, 100 μl/well) was immobilized, and biotin-labeled rVN was used as the soluble ligand to distinguish between the added rVN and the immobilized protein. The bound ligands were detected after incubation with streptavidin-HRP diluted at 1:2000 (v/v) in TBST containing 0.1% BSA and 0.1% Tween 20 for 2 h at 4 °C. Soluble ligands (rVN or rVN(r)) were serially diluted in 0.1% BSA/TBS containing 2 mM $CaCl_2$ and added to the wells. Antibodies recognizing the soluble ligands were diluted to 10 μg/ml in 2% milk/TBST and incubated in the wells for 2 h at room temperature to detect the bound ligands. Detection was facilitated by secondary antibodies (anti-mouse or anti-rabbit IgG-HRP) diluted 1:1000 (v/v) in 2% milk/TBST. In some experiments, biotin-conjugated HA (bHA) (29) was used to test HA binding and was detected by streptavidin-HRP. bHA was added and incubated on the coated substrate, which had been preincubated with rVN (9 μg/ml, 200 μl/well) on microfibrils immobilized to the multiwell plate (2.5 μg/ml, 200 μl/well). bHA was serially diluted 3-fold, beginning with an initial dilution of 5 μg/ml at 200 μl/well. In another experiment, the concentration of rVN used for preincubation was varied (serially diluted 3-fold, beginning with an initial dilution of 9 μg/ml at 200 μl/well), whereas the concentration of bHA (5 μg/ml, 200 μl/well) was maintained constant. Color reactions were achieved using tetramethylbenzidine (Sigma) incubated for 30 min at 25 °C. The absorbance at $A_{370\ nm}$ or $A_{655\ nm}$ was measured using a Benchmark Plus plate reader (Bio-Rad).

Surface Plasmon Resonance—Affinity measurements for versican G1 domain homotypic interaction were calculated from surface plasmon resonance analyses using BIAcore X (BIAcore AB, Uppsala, Sweden). Purified rVN (10 μg/ml) was diluted in 10 mM sodium acetate (pH 4.0), and 1200 response units were coupled to a CM5 sensor chip using an amine coupling kit according to the instructions of the manufacturer. Binding experiments were carried out at a flow rate of 30 μl/min at room temperature. Each sample was diluted in HBS-EP running buffer and injected onto the sensor surface. Several concentrations (5–40 nM) of rVN were flowed over the immobilized rVN or fibrillin-1 rF6 surface. To correct for bulk effects and nonspecific binding, equivalent sample solutions were injected onto untreated sensor surfaces, and the obtained responses were subtracted from the data using an rVN or rF6-immobilized sensor chip. Kinetic parameters were evaluated by BIA evaluation software using steady-state affinity analysis, and equilibrium association constants (K_A (1/M)) and equilibrium dissociation constants (K_D (M)) were calculated. Appropriate immobilization of rVN or rF6 was confirmed by positive response curves when pAb 6084 or mAb69, respectively, was injected.

Tissue Overlay Assays and Immunohistochemistry—Formalin-fixed paraffin-embedded sections from normal human dermis were used in this study. Deparaffinized sections (6-μm-thick sections) were treated with 0.1% saponin for 15 min prior to a blocking treatment for nonspecific binding with 0.1% BSA/PBS for 15 min at room temperature. The samples were then washed with PBS three times for 10 min at room temperature. For immunohistochemistry, the sections were incubated with primary antibodies for 60 min at room temperature, washed in PBS, and incubated with secondary antibodies for another 60 min at room temperature (30). For tissue overlay assays, the sections were incubated with 20 μg/ml rVN in 0.1% BSA/PBS at room temperature for 3 h. Then, the sections were washed with PBS three times, and bound exogenous rVN was specifically detected with FITC-conjugated anti-His (Invitrogen). As a negative control, rVN was omitted from the procedure. Reduced and alkylated rVN was also used as a second negative control. To detect the endogenous G3 domain, mAb 2B1 was used. Endogenous fibrillin-1 and elastin were detected by pAb 9543 and mAb BA4, respectively. Fluorescence-conjugated antibodies (Alexa Fluor 568-conjugated anti-mouse IgG or anti-His mAb together with Alexa Fluor 488-conjugated anti-mouse or anti-rabbit IgG (Invitrogen)) were used to detect primary antibodies or bound ligands.

For the HA binding assay on tissue sections, sections were initially incubated with rVN. Then, 10 μg/ml bHA in 0.1% BSA/TBS containing 2 mM $CaCl_2$ was overlaid at room temperature for 3 h. Sections were washed three times with PBS, and the bound bHA was detected with FITC- or Alexa Fluor 568-conjugated streptavidin (Invitrogen). As a negative control, overlaid ligand was omitted from the procedure.

Electron Microscopy—Pre-embedded EM analyses were performed on buttock skin from a 70-year-old man. The samples were fixed and sectioned. The sections were incubated with pAb 6084, pAb 8531, or mAb 2B1, followed by incubation with 5-nm gold-conjugated secondary antibodies. All EM procedures were performed on a Hanaichi electron microscope (Okazaki, Japan).

Confocal Imaging—Dermal tissue sections were visualized using an LSM 5 EXCITER confocal laser microscope (Carl Zeiss, Oberkochen, Germany) that excluded nonspecific fluorescence from the dermis. Dual-color images were captured in a sequential manner. Negative controls were scanned before sample scanning. Nonspecific fluorescence was not observed in negative controls (absence of primary antibodies or binding ligands (rVN)) using 10% laser power, 720 gain, and −0.50 offset. Subsequently, each sample was scanned using these standard conditions. FITC and Alexa Fluor 568 fluorescent signals were detected at 488- and 543-nm laser excitation, respectively. Dermal specimens were also observed by differential interference contrast and double immunofluorescence imaging. All images were obtained using a ×63× oil-immersion objective. Scanning was performed with a pinhole size of 1.0 airy unit and eight times line averaging. The images were stored in a 512 × 512-pixel, 12-bit TIFF file format and were quantified using ZEN software included with the LSM 5 EXCITER microscope. Images were obtained from three independent tissue specimens, and four clear view areas were chosen from each tissue specimen for quantification. The average of the total fluorescence intensity from 10 areas was quantified.

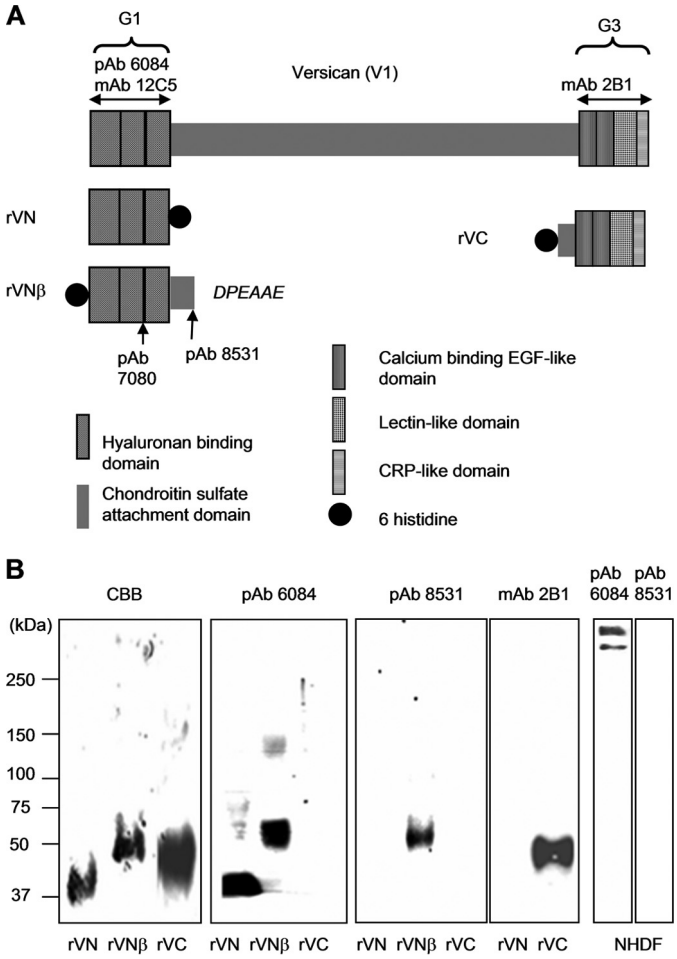

FIGURE 1. **Schematic and characterization of recombinant versican polypeptides and antibodies used in this study.** *A*, schematic of human versican (V1) is shown. Recombinant versican polypeptides, rVN, rVNβ, and rVC are designed as indicated. The recombinant polypeptide rVNβ consists of the G1 domain and the N-terminal portion of the chondroitin sulfate β domain, which ends with the amino acid sequence DPEAAE[441] and represents the cleavage site utilized by ADAMTS-1, ADAMTS-4, and ADAMTS-5. Recognition sites for pAb 6084, pAb 7080, pAb 8531, mAb 12C5, and mAb 2B1 are indicated. *B*, the purified recombinant polypeptides rVN, rVNβ, rVC, and conditioned medium from normal dermal fibroblasts treated with the chondroitinase ABC were subjected to SDS-PAGE under nonreducing conditions and detected by Coomassie Brilliant Blue (*CBB*) and immunoblotting. Antibodies used for detection are indicated at the top. *CRP*, complement regulatory protein.

Statistical Analysis—In all studies, the means ± S.D. were calculated for each group, and statistical analyses of the results were carried out by analysis of variance followed by multiple comparison tests to distinguish between groups.

RESULTS

Characterization of Versican Antibodies and Recombinant Polypeptides—To investigate the biological significance of VG1Fs, we designed and expressed recombinant polypeptides (Fig. 1*A*). In addition to rVN, characterized in our previous study (14), we generated new recombinant polypeptides, rVNβ and rVC. rVNβ was designed to represent the native proteolytic fragment generated by ADAMTS proteases (16). Another new recombinant protein, rVC, was also expressed and purified (Fig.

1, *A* and *B*). As expected, pAb 6084 recognized both rVN and the G1 domain-containing rVN*β*, whereas mAb 2B1 recognized rVC (Fig. 1*B*). Another antiserum, pAb 8531, was raised against the neoepitope DPEAAE, as reported previously (16). Immunoblotting showed that pAb 8531 was specific for rVN*β* (Fig. 1*B*) but did not react with intact versican secreted by NHDFs (*B*). in contrast, pAb 6084 recognized rVN, rVN*β*, and intact versican core protein (Fig. 1*B*).

Extraction of VG1Fs from the Dermis—Immunoblotting and blot overlay assays demonstrated the presence of VG1Fs in dermal extracts. The epitopes for the antibodies used in these experiments are shown in Fig. 1*A*. pAb 6084 (data not shown), pAb 7080 (data not shown), and mAb 12C5 revealed multiple bands present in dermal extracts prepared with 6 M guanidine followed by treatment with chondroitinase ABC (Fig. 2*A*). Bands reacting with pAb 8531, which recognizes the DPEAAE neoepitope in the chondroitin sulfate *β* region, were also identified (Fig. 2*A*), indicating that these molecules were generated by cleavage of versican core protein. A blot overlay analysis with bHA also identified multiple G1 domain-containing bands (Fig. 2*A*). These results demonstrated the presence of cleaved molecules containing the G1 domain (VG1Fs, Fig. 2*A*, *arrows*). Some of the VG1F-containing materials migrated as species larger than 150 kDa (Fig. 2*A*, *asterisk*). However, prominent materials migrated between 50 and 75 kDa (Fig. 2*A*)

To examine the association between VG1Fs and dermal connective tissues in which HA-versican-fibrillin complexes are colocalized (13, 14, 31), sequential extractions were performed. When dermal tissue was extracted with 6 M guanidine solution, multiple pAb 8531-positive bands containing VG1Fs were found in the extract (Fig. 2*B*, *arrows*). After extraction with PBS, the residues were treated with *Streptomyces* HAase. Immunoblotting with pAb 8531 revealed that few, if any, VG1Fs were extracted by these subsequent treatments (Fig. 2*B*). The amount of VG1Fs released from the tissue was not increased by repeated digestion with HAase (data not shown). When the sequential extractions were reversed (dermal tissue was initially extracted with PBS, then with HAase, and finally with 6 M Gdn solution), VG1Fs were not detectable in either the PBS or HAase extracts (Fig. 2*C*). However, pAb 8531-positive materials were released from the residue by further extraction with 6 M Gdn solution (Fig. 2*C*). These results demonstrated that VG1Fs interacted strongly and noncovalently with the dermal extracellular matrix and were not held in the matrix simply through their HA-binding properties alone. In addition, these results suggest that cleavage of versican and release of VG1Fs were likely not due to disruption of the tissue by extraction conditions.

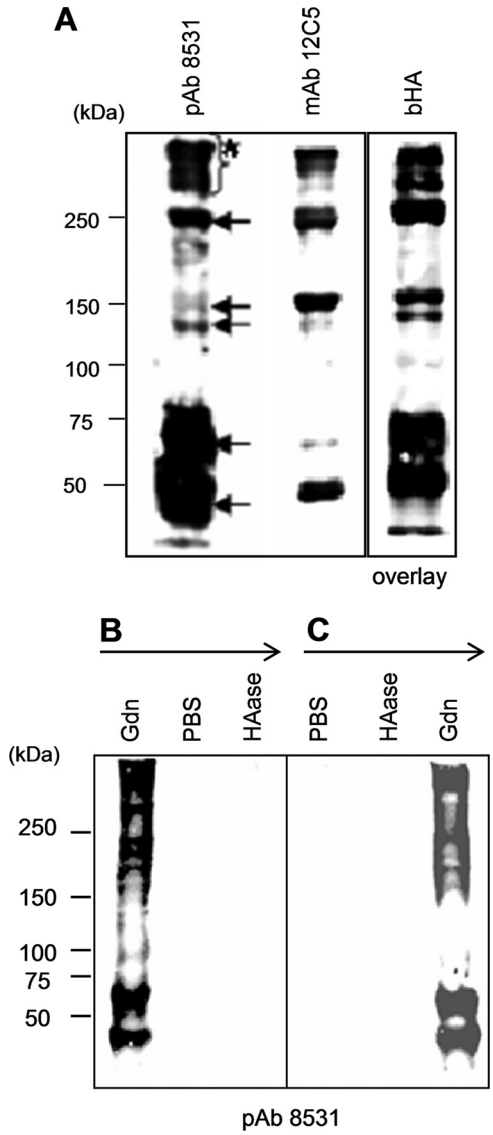

FIGURE 2. **Characterization of VG1Fs from dermal tissue.** *A*, Western blot analyses using anti-versican antibodies and blot overlay assays by bHA. The 6 M guanidine hydrochloride dermal extract was treated with chondroitinase ABC and resolved by SDS-PAGE under nonreducing conditions. The blots were incubated with bHA or specific antibodies as indicated. The blot with pAb 8531 (anti-DPEAAE) showed multiple molecules (*arrows*) containing the bands larger than 150 kDa (*asterisk*) *B* and *C*, Western blot analyses with pAb 8531. The procedures for extraction from the dermis are indicated and are described in detail under "Experimental Procedures." *B*, dermal tissues were sequentially extracted with 6 M guanidine hydrochloride, PBS, and *Streptomyces* HAase treatment. *C*, dermal tissues were sequentially extracted with PBS, *Streptomyces* HAase, and 6 M guanidine hydrochloride. The extracts were precipitated, treated with chondroitinase ABC, resolved on 7.5% acrylamide gels under nonreducing conditions, and blotted.

Exogenous VG1Fs Are Deposited on the Elastic Fiber Network in Dermal Tissue—To examine whether VG1Fs can interact with the elastic fiber network, a tissue overlay assay was performed using the recombinant polypeptides rVN and rVN*β* as soluble ligands. Our results showed that exogenously added rVN was deposited onto fibrous components, *i.e.* the dermal elastic fiber network, where endogenous G3 domains of versican and fibrillin-1 were also present (Fig. 3, *A*, *B*, *D*, and *E*). Colocalization was seen in the merged images (Fig. 3, *C* and *F*). Deposition of rVN was observed in different regions of dermal connective tissue (Fig. 3, *A*, *C*, and *H*), whereas nonspecific staining with secondary antibodies was not observed (*I*). The deposited rVN was also visualized as *red* using differentially labeled antibodies (Fig. 3*J*). The reduced and alkylated rVN did not bind at all to the dermal matrix (Fig. 3*K*). The larger soluble ligand, rVN*β*, also bound to elastic fibers in the dermis (Fig. 3*L*).

VG1Fs Interact with Microfibrils—Because the tissue overlay assay suggested that binding ligands for VG1Fs may be present in elastic fibers, we examined the interaction of the G1 domain with microfibrils. In solid-phase binding assays, rVN specifi-

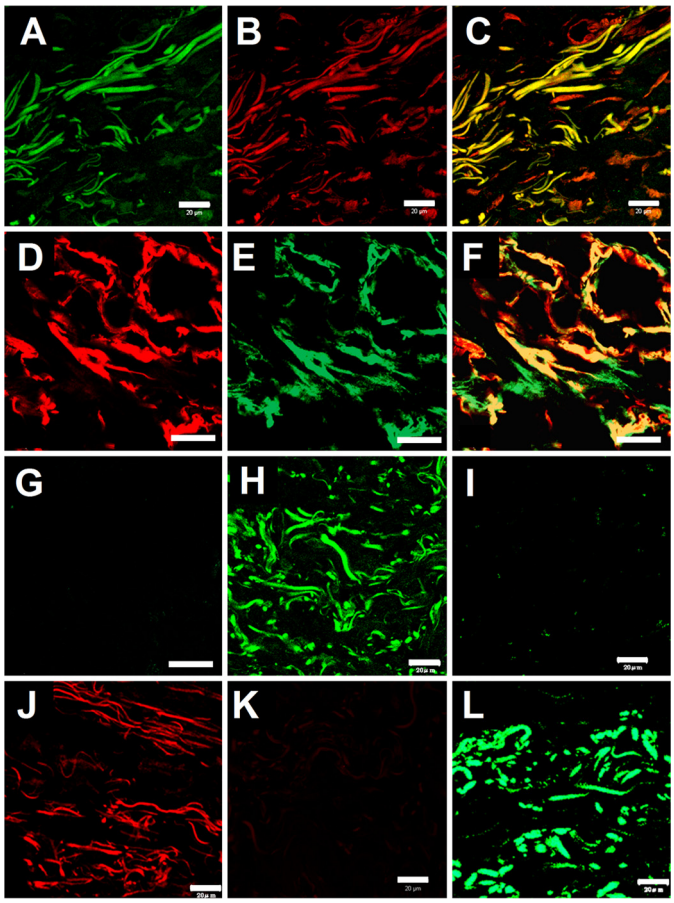

FIGURE 3. **Tissue overlay assays using recombinant VG1Fs.** Dermal sections were overlaid with recombinant versican G1 polypeptides. *A*, bound rVN was detected by FITC-conjugated anti-C-His antibodies (*green*). *B*, the endogenous G3 domain was detected by mAb 2B1 (*red*). *C*, colocalization of the exogenous rVN and endogenous G3 domain is shown in the merged image (*yellow*). *A–C*, *scale bars* = 20 μm. *D*, bound rVN was detected by Alexa Fluor 555-conjugated anti-C-His antibodies (*red*). *E*, endogenous fibrillin-1 was detected by pAb 9543 (*green*). *F*, colocalization of exogenous rVN and endogenous fibrillin-1 is shown in the merged image (*yellow*). *G*, the merged image of a control section (treated similarly but without rVN and pAb 9543) was negative. *D–G*, *scale bars* = 10 μm. *H*, In another field of the section, exogenous rVN was detected (*green*), whereas in I, control sections (treated similarly but without rVN) were negative. *J*, bound rVN (*red*) was also detected by Alexa Fluor 568-conjugated antibodies. *K*, the section overlaid with reduced and alkylated rVN was negative. *L*, exogenously added rVNβ was similarly detected on tissue sections (*green*). *H–L*, *scale bars* = 20 μm.

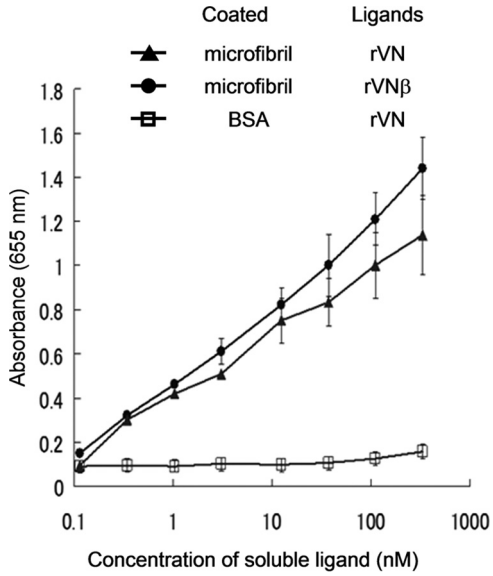

FIGURE 4. **Binding of VG1Fs to extracted microfibrils.** Isolated microfibrils extracted from human fetal membranes or bovine serum albumin (□) were immobilized. Coated microfibrils were prepared using 6 M guanidine extraction, molecular sieve chromatography, and ultracentrifugation containing cesium chloride. rVN (●) and rVNβ (▲) were used as soluble ligands. Each point represents the mean ± S.D. obtained from three independent experiments.

cally interacted with the isolated nondegraded microfibrils from fetal membranes but not with BSA (Fig. 4), indicating the presence of ligands in these preparations of microfibrils. In addition, rVNβ, which represents the G1-containing fragment in normal dermis, bound to the microfibrils (Fig. 4). These microfibril samples did not contain HA because they were purified by ultracentrifugation through a cesium chloride gradient under dissociative condition (26 and data not shown). Moreover, rVN bound to hyaluronidase-treated microfibrils (data not shown). In addition, rVN did not bind to tropoelastin (data not shown).

Versican Is the Major Ligand for VG1Fs in Microfibrils—To determine which molecules in dermal microfibrils interact with rVN, a blot overlay assay was performed using secreted proteins from NHDFs as immobilized ligands. Biotin-conjugated rVN specifically bound to a molecule migrating at ~500 kDa in the secreted proteins treated with chondroitinase ABC (Fig. 5*A*). In contrast, the corresponding band was not observed in samples without chondroitinase ABC treatment (Fig. 5*A*), indicating that either rVN interacts with the core protein of chondroitin sulfate proteoglycans or that the interacting protein binds to chondroitin sulfate proteoglycans, which would not enter the gel without removal of the side chains. Immunoblotting with pAb 6084 indicated that the versican core protein, migrating at ~500 kDa, was a possible ligand for rVN (Fig. 5*A*). Bound rVN was also detected at ~500 kDa using HRP-conjugated anti-hexahistidine antibodies (Fig. 5*B*). Hyaluronidase treatment for rVN and/or secreted proteins from NHDFs did not interfere with the binding (data not shown). However, when the medium proteins from NHDFs were reduced, no binding was observed (Fig. 5*B*), suggesting that the globular domains at both ends of the versican core protein were candidates for the binding site. A band migrating around 350 kDa, corresponding to the size of the fibrillin-1 monomer (10), was not observed in the assay.

Using dermal guanidine extracts as immobilized ligands, rVN bound to multiple molecules migrating in the range of 40 – 400 kDa (Fig. 5*C*). The band patterns were almost identical to those detected by Western blotting with pAb 6084 (Fig. 5*C*). In contrast, the most prominent band detected by mAb 2B1 was found to be migrating at ~500 kDa, most likely corresponding to the versican monomer (Fig. 5*C*). Other smaller bands detected by rVN overlay and by pAb 6084 lacked the C-terminal mAb 2B1 epitope. These results suggest that rVN can bind to VG1Fs extracted from the dermis.

Homotypical Interactions of the Globular Domains of Versican—Interactions of VG1Fs were further tested using solid-phase binding assays. rVN specifically bound to the intact proteoglycan form of versican purified from conditioned medium from NHDFs (Fig. 6*A*) (19), confirming our results

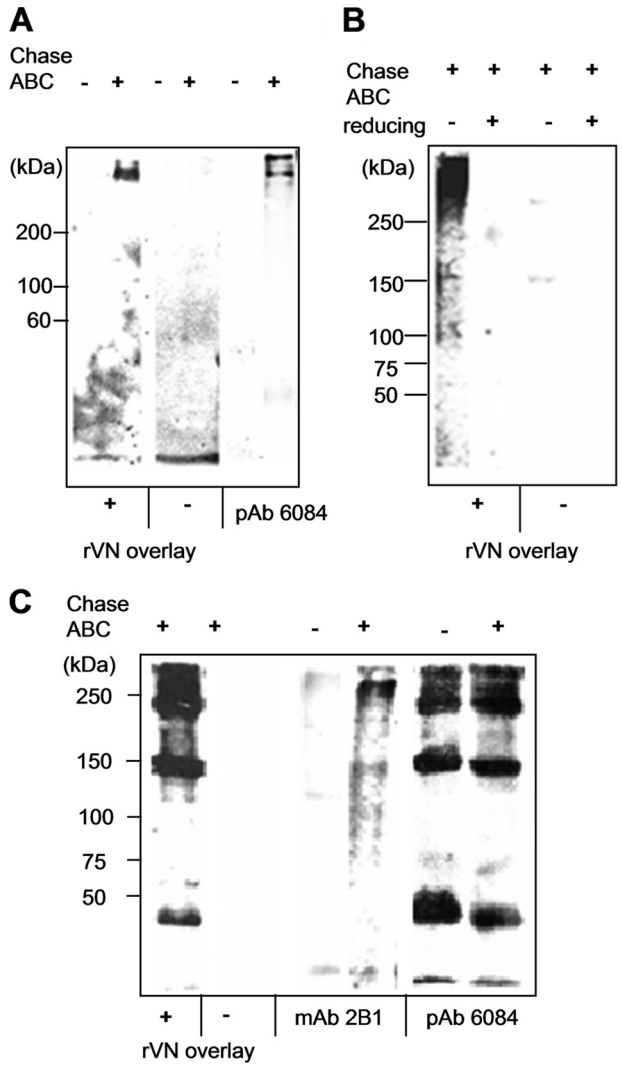

FIGURE 5. **The presence of ligands for rVN in secreted molecules from dermal fibroblasts and in dermal extracts.** To identify ligands for rVN, blot overlay assays were performed. Conditioned medium from NHDFs (*A* and *B*) and dermal extracts, prepared using 6 M guanidine hydrochloride (*C*) with (+) or without (-) chondroitinase ABC treatment, were resolved and blotted. *A*, biotin-conjugated rVN was used as the soluble ligand. bound rVN was detected by HRP-conjugated avidin. Western blot analysis using pAb 6084 (anti-G1) is shown, indicating the migration of the versican core protein. *B*, anti-His antibodies were used for detection of bound rVN. The samples were run under nonreducing (-) or reducing (+) conditions. *C*, the dermal extract was the immobilized ligand. Biotin-conjugated rVN was used as the soluble ligand. Western blot analyses using pAb 6084 and mAb 2B1 (Fig. 1) showed species containing N-terminal and C-terminal domains of versican present in dermal extracts.

from the blot overlay assay. These results suggested that chondroitin sulfate chains of versican did not interfere with the interaction. As a negative control, the reduced and alkylated rVN did not bind to versican (Fig. 6*A*). In addition, rVN did not bind to recombinant fibrillin-1 fragments rF11 and rF6 (Fig. 6*B*), consistent with the results of the blot overlay analysis.

Because rVN did not bind to the reduced versican core protein (Fig. 5*B*), we next tested the interactions between the globular domains. Biotin-conjugated rVN bound to both rVN and rVC immobilized on wells (Fig. 6*C*). By surface plasmon resonance using BIAcore, self-association of rVN was observed at each concentration (Fig. 6*D*). For the self-interaction of rVN, the dissociation constant K_D (K_d/K_a) was 95.8 nM, suggesting moderately strong self-interaction of the versican G1 domain. In contrast, the control ligand rF6 (the carboxyl-terminal half of fibrillin-1) showed no binding to rVN when rF6 was immobilized on the sensor chip (Fig. 6*E*).

VG1Fs Formed Macroaggregates in the Dermis—Extraction experiments demonstrated that VG1Fs migrated as species larger than 100 kDa and that the mobilities of the molecules were not markedly affected by chondroitinase ABC treatment (Fig. 2*C*). Moreover, our results demonstrated the homotypical interaction of rVN. Therefore, we sought to further define high molecular weight aggregates containing VG1Fs in dermal tissue. Dermal tissue was extracted with 6 M guanidine, and the soluble extracts were sieved on Sepharose CL-2B under dissociative conditions. Immunoreactivity with pAb 8531, recognizing the DPEAAE neoepitope sequence, was detected in the void volume fractions as well as in fractions that eluted later (Fig. 7*A*). Because the neoepitope DPEAAE is generated after cleavage by ADAMTS proteases (16, 17) and because pAb 8531 specifically reacted with the cleavage site of chondroitin sulfate β of versican but not with intact versican core protein (Fig. 1*B*), it is likely that VG1Fs may form large aggregates in the dermis. Consistent with these findings, void volume aggregates reacted positively with pAb 6084 (anti-G1) and pAb 7080 (anti-G1) but not with mAb 2B1 (anti-G3), pAb 9543 (anti-fibrillin-1), or mAb 8A4 (anti-link protein, Fig. 7*A* and data not shown). Interestingly, the aggregates bound to soluble rVN and bHA during blot overlay analysis (Fig. 7*A*). In contrast, rVN(r) (reduced and alkylated rVN) and HABP did not bind to the aggregates. These results suggested that VG1F aggregates were capable of binding to the versican G1 domain and HA.

For further characterization of VG1F-containing macroaggregates, void volume fractions were isolated by ultracentrifugation in cesium chloride. The pAb 6084-positive fraction was visualized by electron microscopy after rotary shadowing. Morphological analysis of VG1F-containing aggregates revealed a polygonal shape, with aggregates ranging from 5 to 25 nm in diameter (Fig. 7*B*). Microfibrils were not observed in any preparation. Then, the aggregates were treated with trypsin alone or trypsin and V8 protease and subjected to SDS-PAGE. Subsequent protein staining and immunoblotting with pAb 6084 indicated that the versican G1 domain was a major constituent of the aggregates (Fig. 7*C*).

Consistent with biochemical results, immunoelectron microscopic imaging with pAb 6084 demonstrated that gold labeling could be observed on microfibril structures. The gold labeling appeared to be aggregated either to microfibrils around the amorphous elastin core or to microfibrils positioned away from the elastin core (Fig. 8, *A* and *B*). Occasionally, labeling was observed in the region independent of microfibrils. Similarly, immunolocalization with pAb 8531, an anti-DPEAAE antibody, was identical to that with pAb 6084 (Fig. 8, *C* and *D*), indicating that VG1Fs were localized to microfibrils in adult dermis. However, periodic labeling, like that of fibrillin-1, was not observed. Immunolocalization with mAb 2B1 (Fig. 8*E*) was shown, as reported previously (8). No labeling with nonimmune serum was observed (Fig. 8*F*).

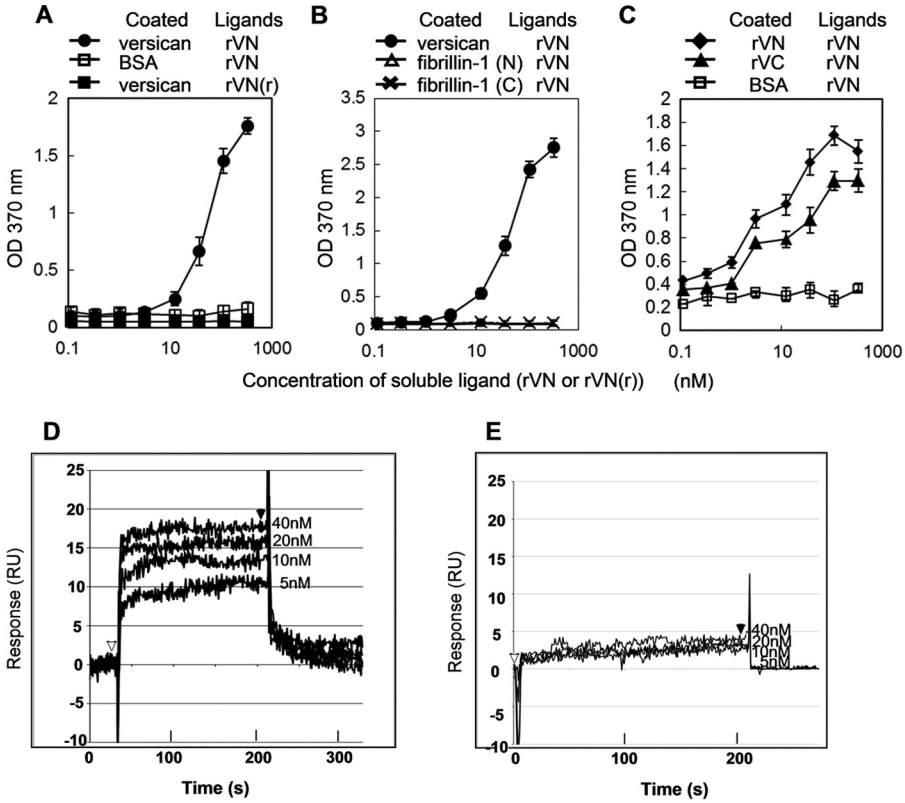

FIGURE 6. **Interactions of recombinant globular domains of versican.** Solid-phase binding assays were performed using rVN as a soluble ligand (*A–C*). *A*, native versican purified from NHDF (●) or BSA (□) was immobilized. Reduced and alkylated rVN (■) was also used as a negative control (indicated as rVN(r)). *B*, native versican, fibrillin-1 (*N*) (rF11, fibrillin-1 amino-terminal half), or fibrillin-1 (*C*) (rF6, fibrillin-1 carboxyl-terminal half) was used to coat wells. Soluble rVN bound to native versican (●). In contrast, rVN did not bind to fibrillin-1 (△) or fibrillin-1 (*C*) (×). *C*, biotin-conjugated rVN bound to wells coated with rVN (♦) and to rVC (recombinant G3 domain, ▲) but not to BSA (□). Binding of soluble biotin-conjugated rVN to immobilized BSA was used as a negative control. Each point in *A–C* is the mean ± S.D. obtained from three independent experiments. *D* and *E*, BIAcore sensorgrams of rVN interactions. Experiments were performed with a series of titrated analytes (rVN) in solution with the indicated concentrations, flowed over a CM5 sensor chip immobilized with 1200 RU of rVN (*D*) or rF6 (*E*). The analytes were injected at the point indicated by △, and the dissociation phase began at the point indicated by ▲. *RU*, resonance unit.

VG1Fs Enhanced Recruitment of HA to Microfibrils—To clarify the roles of VG1Fs in HA recruitment to microfibrils, HA-binding assays were performed in the presence of exogenous rVN. Because the microfibrils used in this assay included intact versican molecules containing the G1 and G3 domains (data not shown), bHA bound to the coated microfibrils (Fig. 9*A*, ■). When rVN was preincubated with the immobilized microfibrils, HA binding to microfibrils increased at all concentrations of bHA (Fig. 9*A*, ●). Moreover, the amount of bound HA was dependent on the amount of added rVN at a constant concentration of HA (Fig. 9*B*).

The effects of exogenous VG1Fs on HA recruitment to microfibrils was also examined by a tissue overlay assay using bHA as the soluble ligand. When rVN was preincubated with the dermal tissue specimens, the deposition of HA around elastic fibers was increased significantly (Fig. 9*D* and data not shown) compared with control specimens (*C*). Quantifying the images clarified the increase of fluorescence intensity in the presence of exogenous rVN (Fig. 9*E*).

DISCUSSION

In this study, we clarified the structural properties of versican fragments containing the G1 domain and VG1Fs in the HA-microfibril network in the dermis, where HA-versican-microfibril complexes are associated, and demonstrated that VG1Fs homotypically interacted with and incorporated HA into dermal microfibrils.

Consistent with our previous study (14), VG1Fs were found in 6 M guanidine extracts from the dermis. In contrast, hyaluronidase treatment released only small quantities of pAb 8531-positive molecules, indicating that VG1Fs were not simply associated with dermal ECMs through their preserved HA-binding properties. Therefore, it seems likely that VG1Fs require protein ligands to localize to the fibrillin microfibril network in the normal dermis.

Microfibrils are ubiquitous connective tissue elements composed of fibrillins and other associated proteins such as fibulins, microfibril-associated glycoproteins, versican, LTBP-1 (latent TGF beta-binding protein 1), and LTBP-4 (6–8, 25, 27, 32, 33). Our unique tissue overlay assay revealed that exogenous rVN was deposited onto the dermal elastic fiber network, where the G3 domain of versican is localized (5, 14), and could bind to extracted fibrillin microfibrils, suggesting that VG1Fs could be recaptured by microfibrils. In addition, our tissue overlay assay showed that binding ligands for VG1Fs were available in the dermal connective tissues. By using blot overlay assays, versican core protein, but not fibrillin-1, was shown to be a novel ligand for VG1Fs. In addition, our results also indicated that other molecules, including chondroitin sulfate chains, LTBPs, fibu-

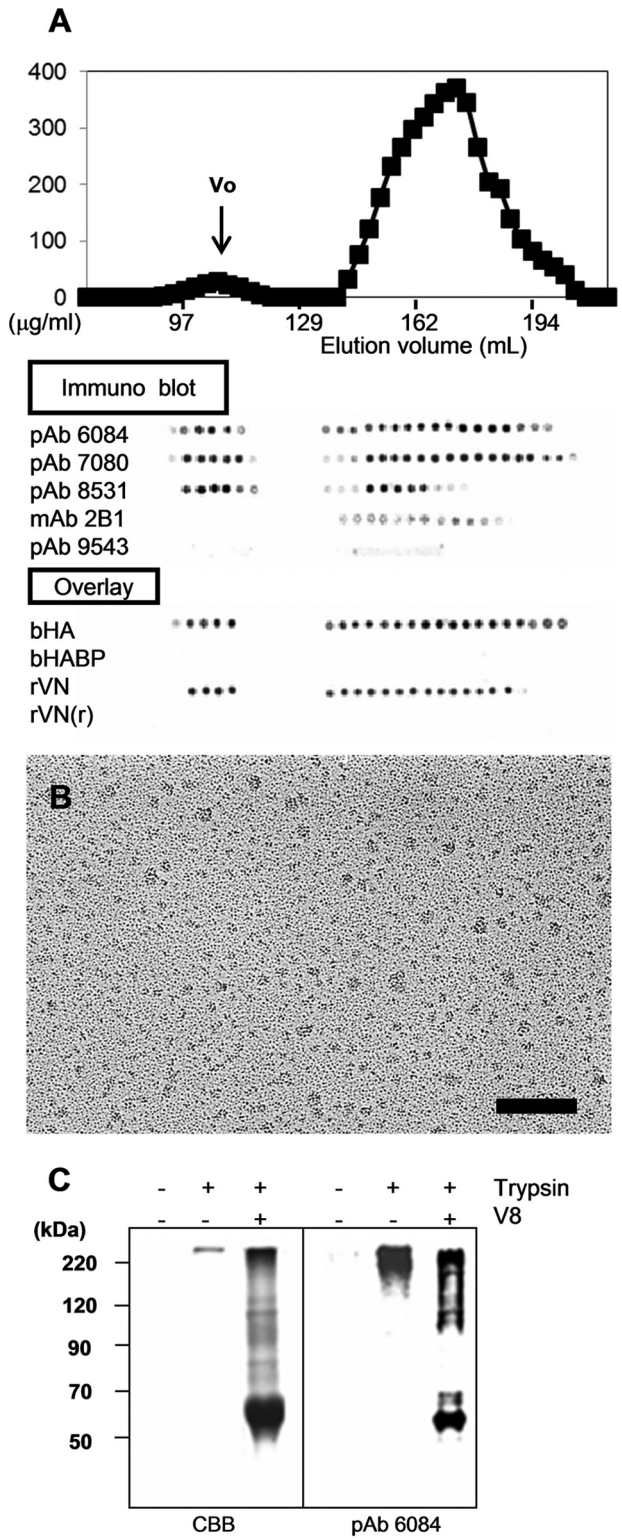

FIGURE 7. **Identification of VG1F-containing aggregates in dermal extracts.** *A*, dermal tissues were extracted with a 6 M guanidine solution. The extract was concentrated using a 50-kDa molecular mass cutoff membrane and sieved on Sepharose CL-2B columns under dissociative conditions. Protein concentrations (micrograms/milliliters), dot blot analyses, and overlay assays using rVN and bHA as soluble ligands are shown. Antibodies used for dot blot analyses are indicated. The void volume fractions were positive with pAb 8531 (neoepitope, DPEAAE) and pAb 7080 (anti-G1 domain) but not with anti-G3 domain antibodies (mAb 2B1) or anti fibrillin-1 antibodies (pAb 9543). Blot overlay analyses using rVN, rVN(r), biotin-conjugated HABP (*bHABP*), and bHA are also shown. The void fractions bound to rVN and bHA but were negative for rVN(r) and HABP. *B*, rotary shadowed electron microscopy of VG1F-containing aggregates is shown. The pAb 6084 positive-void volume fractions from sieved chromatography (*A*) were further isolated by ultracentrifugation containing cesium chloride. *Scale bar* = 100 nm. *C*, analysis of the fractions shown in *B*. Fractions were treated with trypsin alone or trypsin and V8 protease. The samples were resolved by SDS-PAGE, analyzed by staining with Coomassie Brilliant Blue (*CBB*), and immunoblotting with pAb 6084 (anti-G1).

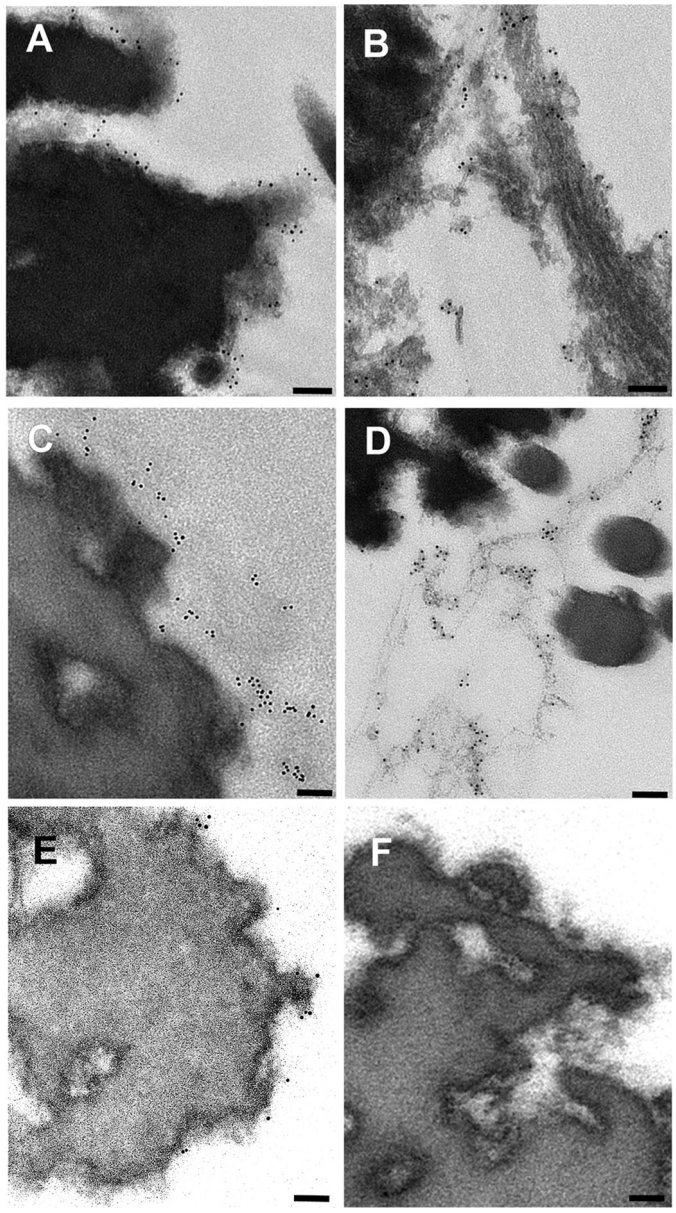

FIGURE 8. **Immunoelectron microscopic localization of the versican G1 domain in the dermal connective tissue.** In human adult dermis, pAb 6084 was used to label the versican G1 domain with gold (*A* and *B*). The dermis was also incubated with the neoepitope antibody pAb 8531 (*C* and *D*) and the anti-versican G3 antibody mAb 2B1 (*E*). Incubation with nonimmune rabbit serum was performed as a control (*F*). *Scale bars* = 100 nm.

lins, and other associated molecules, did not inhibit the binding of VG1Fs.

Because the binding of VG1Fs to versican core protein was abolished under reducing conditions, the globular domains containing disulfide bonds were the likely binding sites for rVN. Using recombinant versican globular domains, homotypic

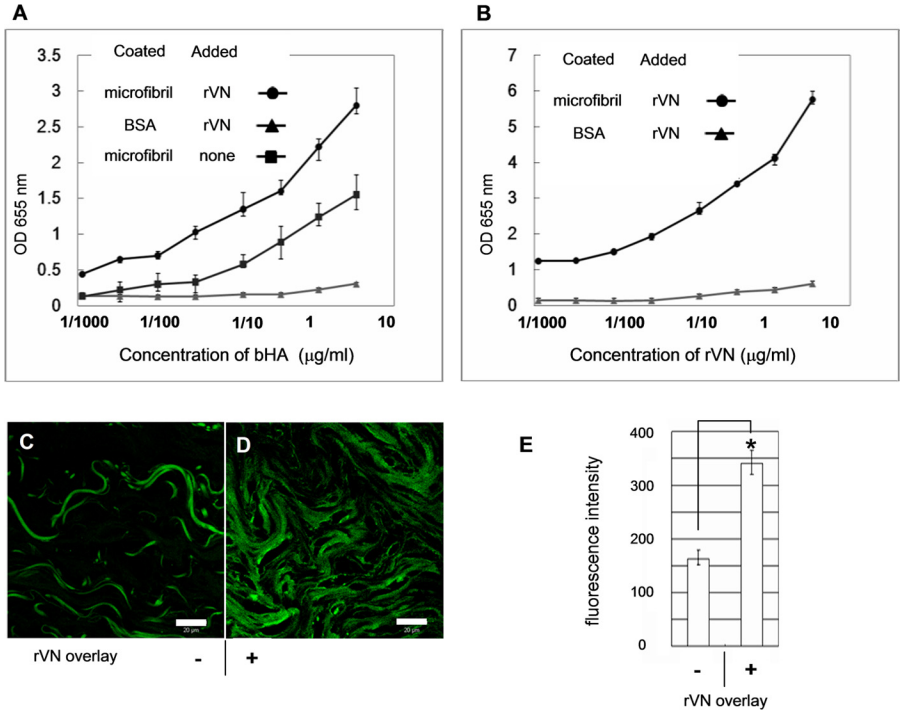

FIGURE 9. **Exogenous versican G1 fragments enhance HA deposition into microfibrils.** Solid-phase binding assays were performed using bHA as a soluble ligand and immobilized microfibrils bound with rVN (*A* and *B*). *A*, before incubation with hyaluronan, the immobilized microfibrils were incubated with rVN at a constant concentration of 9 μg/ml (●). Binding of bHA was enhanced by the preincubation of exogenous rVN compared with microfibrils without preincubated rVN (■). bHA did not bind to the coated BSA preincubated with rVN (▲). *B*, solid-phase binding assay using bHA as a soluble ligand at a constant concentration (5 μg/ml). Immobilized microfibrils or BSA were preincubated with increasing concentrations of rVN. *C* and *D*, tissue overlay assay using bHA (*green*) as a soluble ligand on dermal tissue preincubated without rVN (*C*) or with rVN (*D*). *Scale bars* = 20 μm. *E*, quantification of the fluorescence intensity from images similar to *C* and *D* resulted in significant differences (*, $p = 0.0067$) between tissue sections treated with rVN compared with control untreated tissue sections. The *error bar* represents the mean ± S.D. fluorescence intensity obtained from 10 areas.

interactions of versican G1 domain were demonstrated, consistent with blot overlay assays in which rVN bound to pAb 6084-positive molecules. This binding was also confirmed by surface plasmon resonance. Fibrillin-1, although a major constituent of microfibrils, was not a ligand for VG1Fs. However, through intact versican bound to microfibrils (8, 15), VG1Fs can be recaptured by microfibrils. Taken together, these data suggested that VG1Fs could accumulate on microfibrils through homotypic interactions of versican globular domains (Fig. 10*B*).

Consistent with homotypic binding, macroaggregates containing VG1Fs were identified in the dermal extracts. In contrast, lack of immunoreactivities with the anti-G3 domain and anti-fibrillin-1 antibodies suggested that the macroaggregates found in this study were different from the versican-bound microfibrils detected previously (8, 15). This result also suggested that the noncovalent G1-G3 interaction may not be responsible for formation of macroaggregates containing VG1Fs. Because we used 6 M guanidine to extract the aggregates and isolated them under dissociative conditions, this method allowed us to find macroaggregates that had not been reported in previous studies (20). Therefore, it can be speculated that cleavage by ADAMTS proteases is a critical step for forming VG1Fs macroaggregates. Rotary shadowing and electron microscopy demonstrated the morphological characteristics of VG1F macroaggregates, and immunoblotting of protease-treated fragments demonstrated that the major components of the macroaggregates were VG1Fs. Furthermore, VG1F multimers bound to additional rVN and HA by overlay analyses, suggesting that the binding sites for VG1Fs and HA were available in the VG1F macroaggregates. Consistent with the biochemical properties of these proteins, isolated VG1F containing macroaggregates exhibited a wide range of diameters after rotary shadowing and EM. Moreover, although it has been reported that link protein is expressed in chicken embryonic dermis and binds to versican (34, 35), our results demonstrated that link protein was not a constituent of VG1F multimers, nor a major ligand for VG1Fs in the adult dermis.

The binding properties of the G1 domain of versican, aggrecan, and link protein to HA were characterized using recombinant proteins (35–38), and interactions between those HA binding regions were shown. However, until now, homotypic interactions of VG1Fs have not been reported. On the basis of the assumption of lack of homotypic interaction of VG1Fs, we initially speculated that VG1Fs would competitively disrupt HA recruitment to microfibrils. Contrary to our expectations, our results showed that exogenous addition of rVN enhanced HA incorporation into microfibrils. In cartilage, link protein stabilizes the HA-aggrecan matrix (39). However, the role of link proteins or similar molecules in the dermis has not yet been reported. In this study, our data suggest that the aggregative properties of VG1Fs may facilitate the incorporation of VG1Fs and HA into the matrix in dermal tissues. Thus, VG1Fs could possess a stabilizing role similar to the role of link proteins in cartilage (Fig. 10*B*).

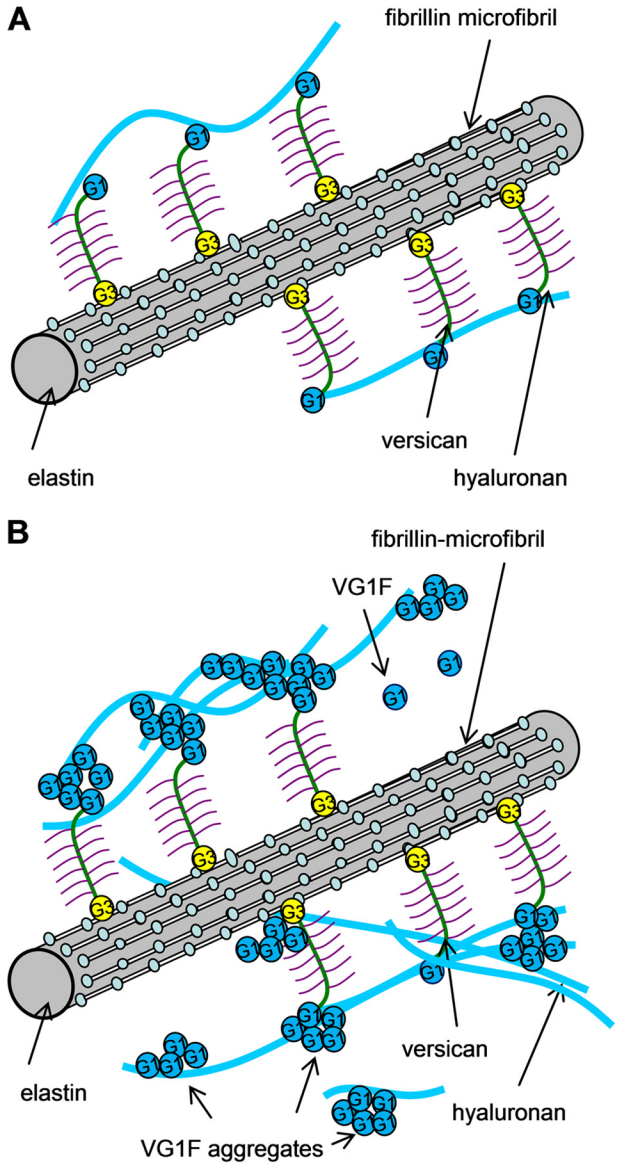

FIGURE 10. **Proposed model for the hyaluronan-microfibril complex mediated by homotypic interaction of VG1Fs.** *A*, Because intact versican binds to HA using its amino-terminal G1 domain, HA is linked to microfibrils through versican molecules by a model identified previously. *B*, cleavage of the intact versican generates VG1Fs. VG1Fs interact homotypically and with the G1 or G3 domain of versican attached to microfibrils. Consequently, cleaved and recaptured VG1Fs can enhance recruitment of HA to microfibrils.

Recently, proteolysis of versican by ADAMTS proteases has been shown to play key biological roles in ovulation (40), neointimal atrophy (41), interdigital web regression (42), and palatal mesenchyme proliferation (43). Dermal fibroblasts that are deficient in ADAMTS-5 exhibit a myofibroblastic phenotype (44), and transfection of cancer cells with the versican G1 domain exaggerates tumor progression (45). However, the mechanisms mediating these activities and whether versican cleavage products perform important roles are not fully understood. The results of this study show that VG1Fs can interact with HA and with versican globular domains, suggesting that versican cleavage products can perform important functional roles. Furthermore, we now know that the versican-microfibril complex can sequester VG1Fs within the microfibril network, forming a specific depot of biologically active VG1Fs positioned to recruit HA. We propose that VG1F macroaggregates can capture more HA onto microfibrils when needed. The potentially dynamic interactions of VG1Fs may be a fundamental structural property of the fibrillin-versican-HA complex in connective tissue, as depicted in Fig. 10. Disruption of any part of this network could compromise the structural and functional integrity of connective tissue and might explain certain effects of ADAMTS protease deficiency on connective tissue function.

Acknowledgments—We thank Dr. Ko Tsutsui for help with the binding assays for which BIAcore instrumentation was used.

REFERENCES

1. Feinberg, T., and Weiss, S. J. (2009) Developmental ECM sculpting. Laying it down and cutting it up. *Dev. Cell.* **17,** 584–586
2. Kimata, K., Oike, Y., and Tani, K., Shinomura, T., Yamagata, M., Uritani, M., and Suzuki S. (1986) A large chondroitin sulfate proteoglycan (PG-M) synthesized before chondrogenesis in the limb bud of chick-embryo. *J. Biol. Chem.* **261,** 13517–13525
3. Zimmermann, D. R., and Ruoslahti, E. (1989) Multiple domains of the large fibroblast proteoglycan, versican. *EMBO J.* **8,** 2975–2981
4. LeBaron, R. G., Zimmermann, D. R., and Ruoslahti, E. (1992) Hyaluronate binding-properties of versican. *J. Biol. Chem.* **267,** 10003–10010
5. Zimmermann, D. R., Dours-Zimmermann, M. T., Schubert, M., and Bruckner-Tuderman, L. (1994) Versican is expressed in the proliferating zone in the epidermis and in association with the elastic network of the dermis. *J. Cell Biol.* **124,** 817–825
6. Aspberg, A., Adam, S., Kostka, G., Timpl, R., and Heinegård, D. (1999) Fibulin-1 is a ligand for the C-type lectin domains of aggrecan and versican. *J. Biol. Chem.* **274,** 20444–20449
7. Olin, A. I., Mörgelin, M., Sasaki, T., Timpl, R., Heinegård, D., and Aspberg, A. (2001) The proteoglycans aggrecan and versican form networks with fibulin-2 through their lectin domain binding. *J. Biol. Chem.* **276,** 1253–1261
8. Isogai, Z., Aspberg, A., Keene, D. R., Ono, R. N., Reinhardt, D. P., and Sakai, L. Y. (2002) Versican interacts with fibrillin-1 and links extracellular microfibrils to other connective tissue networks. *J. Biol. Chem.* **277,** 4565–4572
9. Keene, D. R., Maddox, B. K., Kuo, H. J., Sakai, L. Y., and Glanville, R. W. (1991) Extraction of extendable beaded structures and their identification as fibrillin-containing extracellular-matrix microfibrils. *J. Histochem. Cytochem.* **39,** 441–449
10. Sakai, L. Y., Keene, D. R., and Engvall, E. (1986) Fibrillin, a new 350-kD glycoprotein, is a component of extracellular microfibrils. *J. Cell Biol.* **103,** 2499–2509
11. Handford, P. A., Downing, A. K., Reinhardt, D. P., and Sakai, L. Y. (2000) Fibrillin. From domain structure to supramolecular assembly. *Matrix Biol.* **19,** 457–470
12. Charbonneau, N. L., Carlson, E. J., Tufa, S., Sengle, G., Manalo, E. C., Carlberg, V. M., Ramirez, F., Keene, D. R., and Sakai, L. Y. (2010) *In vivo* studies of mutant fibrillin-1 microfibrils. *J. Biol. Chem.* **285,** 24943–24955
13. Bode-Lesniewska, B., Dours-Zimmermann, M. T., Odermatt, B. F., Briner, J., Heitz, P. U., and Zimmermann, D. R. (1996) Distribution of the large aggregating proteoglycan versican in adult human tissues. *J. Histochem. Cytochem.* **44,** 303–312
14. Hasegawa, K., Yoneda, M., Kuwabara, H., Miyaishi, O., Itano N, Ohno, A., Zako, M., and Isogai, Z. (2007) Versican, a major hyaluronan-binding component in the dermis, loses its hyaluronan-binding ability in solar elastosis. *J. Invest. Dermatol.* **127,** 1657–1663
15. Ohno-Jinno, A., Isogai, Z., Yoneda, M., Kasai, K., Miyaishi, O., Inoue, Y., Kataoka, T., Zhao, J. S., Li, H., Takeyama, M., Keene, D. R., Sakai, L. Y., Kimata, K., Iwaki, M., and Zako, M. (2008) Versican and fibrillin-1 form a major hyaluronan-binding complex in the ciliary body. *Invest. Ophthal-*

mol. Vis. Sci. **49,** 2870–2877
16. Sandy, J. D., Westling, J., Kenagy, R. D., Iruela-Arispe, M. L., Verscharen, C., Rodriguez-Mazaneque, J. C., Zimmermann, D. R., Lemire, J. M., Fischer, J. W., Wight, T. N., and Clowes, A. W. (2001) Versican V1 proteolysis in human aorta *in vivo* occurs at the Glu-441-Ala-442 bond, a site that is cleaved by recombinant ADAMTS-1 and ADAMTS-4. *J. Biol. Chem.* **276,** 13372–13378
17. Apte SS (2009) A disintegrin-like and metalloprotease (reprolysin-type) with thrombospondin type 1 motif (ADAMTS) superfamily: functions and mechanisms. *J. Biol. Chem.* **284,** 31493–31497
18. Halpert I., Sires U. I., Roby J. D., Potter-Perigo S., Wight T. N., Shapiro S. D., Welgus H. G., Wickline S. A., Parks W. C. (1996) Matrilysin is expressed by lipid-laden macrophages at sites of potential rupture in atherosclerotic lesions and localizes to areas of versican deposition, a proteoglycan substrate for the enzyme. *Proc. Natl. Acad. Sci. U.S.A.,* **93,** 9748–9753
19. Sorrell, J. M., Carrino, D. A., Baber, M. A., and Caplan, A. I. (1999) Versican in human fetal skin development. *Anat. Embryol.* **199,** 45–56
20. Carrino, D. A., Calabro, A., Darr, A. B., Dours-Zimmermann, M. T., Sandy, J. D., Zimmermann, D. R., Sorrell, J. M., Hascall, V. C., and Caplan, A. I. (2011) Age-related differences in human skin proteoglycans. *Glycobiology* **21,** 257–268
21. Perides, G., Lane, W. S., Andrews, D., Dahl, D., and Bignami, A. (1989) Isolation and partial characterization of a glial hyaluronate-binding protein. *J. Biol. Chem.* **264,** 5981–5987
22. Isogai, Z., Shinomura, T., Yamakawa, N., Takeuchi, J., Tsuji, T., Heinegård, D., and Kimata, K. (1996) 2B1 antigen characteristically expressed on extracellular matrices of human malignant tumors is a large chondroitin sulfate proteoglycan, PG-M/versican. *Cancer Res.* **56,** 3902–3908
23. Pereira, L., Andrikopoulos, K., Tian, J., Lee, S. Y., Keene, D. R., Ono, R., Reinhardt, D. P., Sakai, L. Y., Biery, N. J., Bunton, T., Dietz, H. C., and Ramirez, F. (1997) Targetting of the gene encoding fibrillin-1 recapitulates the vascular aspect of Marfan syndrome. *Nat. Genet.* **17,** 218–222
24. Neame, P. J., Périn, J. P., Bonnet, F., Christner, J. E., Jollès, P., and Baker, J. R. (1985) An amino-acid sequence common to both cartilage proteoglycan and link protein. *J. Biol. Chem.* **260,** 12402–12404
25. Reinhardt, D. P., Sasaki, T., Dzamba, B. J., Keene, D. R., Chu, M.-L., Göhring, W., Timpl, R., and Sakai, L. Y. (1996) Fibrillin-1 and fibulin-2 interact and are colocalized in some tissues. *J. Biol. Chem.* **271,** 19489–19496
26. Kuo, C.-L., Isogai, Z., Keene, D. R., Hazeki, N., Ono, R. N., Sengle, G., Bächinger, H. P., and Sakai, L.Y. (2007) Effects of fibrillin-1 degradation on microfibril ultrastructure. *J. Biol. Chem.* **282,** 4007–4020
27. Isogai, Z., Ono R. N., Ushiro, S., Keene, D. R., Chen, Y., Mazzieri, R., Charbonneau N. L., Reinhardt D. P., Rifkin D.B., and Sakai L.Y. (2003) Latent transforming growth factor β-binding protein 1 interacts with fibrillin and is a microfibril-associated protein. *J. Biol. Chem.* **278,** 2750–2757
28. Crestfield, A. M., Moore, S., and Stein, W. H. (1963) The preparation and enzymatic hydrolysis of reduced and *S*-carboxymethylated proteins. *J. Biol. Chem.* **238,** 622–627
29. Inoue, Y., Yoneda, M., Zhao, J., Miyaishi, O., Ohno-Jinno, A., Kataoka, T., Isogai, Z., Kimata, K., Iwaki, M., and Zako, M. (2006) Molecular cloning and characterization of chick SPACRCAN. *J. Biol. Chem.* **281,** 10381–10388
30. Murasawa, Y., Hayashi, T., and Wang, P.-C. (2008) The role of type V collagen fibril as an ECM that induces the motility of glomerular endothelial cells. *Exp. Cell Res.* **314,** 3638–3653
31. Bernstein, E. F., Fisher, L. W., Li, K., LeBaron, R. G., Tan, E. M., and Uitto, J. (1995) Differential expression of the versican and decorin genes in photoaged and sun-protected skin. Comparison by immunohistochemical and northern analyses. *Lab. Invest.* **72,** 662–669
32. Gibson, M. A., Hughes, J. L., Fanning, J. C., and Cleary, E. G. (1986) The major antigen of elastin-associated microfibrils is a 31-kDa glycoprotein. *J. Biol. Chem.* **261,** 11429–11436
33. Ono, R. N., Sengle, G., Charbonneau, N. L., Carlberg, V., Bächinger, H. P., Sasaki, T., Lee-Arteaga, S., Zilberberg, L., Rifkin, D. B., Ramirez, F., Chu, M. L., and Sakai, L. Y. (2009) Latent transforming growth factor β-binding proteins and fibulins compete for fibrillin-1 and exhibit exquisite specificities in binding sites. *J. Biol. Chem.* **284,** 16872–16881
34. Binette, F., Cravens, J., Kahoussi, B., Haudenschild, D. R., and Goetinck, P.F. (1994) Link protein is ubiquitously expressed in non-cartilaginous tissues where it enhances and stabilizes the interaction of proteoglycans with hyaluronic-acid. *J. Biol. Chem.* **269,** 19116–19122
35. Matsumoto, K., Shionyu, M., Go, M., Shimizu, K., Shinomura, T., Kimata, K., and Watanabe, H. (2003) Distinct interaction of versican/PG-M with hyaluronan and link protein. *J. Biol. Chem.* **278,** 41205–41212
36. Day, A. J., and Prestwich, G. D. (2002) Hyaluronan-binding proteins. *J. Biol. Chem.* **277,** 4585–4588
37. Shi, S., Grothe, S., Zhang, Y., O'Connor-McCourt, M. D., Poole, A. R., Roughley, P. J., and Mort J. S. (2004) Link protein has greater affinity for versican than aggrecan. *J. Biol. Chem.* **279,** 12060–12066
38. Seyfried, N. T., McVey, G. F., Almond, A., Mahoney, D. J., Dudhia, J., and Day, A. J. (2005) Expression and purification of functionally active hyaluronan-binding domains from human cartilage link protein, aggrecan and versican. Formation of ternary complexes with defined hyaluronan oligosaccharides. *J. Biol. Chem.* **280,** 5435–5448
39. Watanabe, H., Yamada, Y., and Kimata, K. (1998) Roles of aggrecan, a large chondroitin sulfate proteoglycan, in cartilage structure and function. *J. Biochem.* **124,** 687–693
40. Russell, D. L., Doyle, K. M., Ochsner, S. A., Sandy, J. D., and Richards, J. S. (2003) Processing and localization of ADAMTS-1 and proteolytic cleavage of versican during cumulus matrix expansion and ovulation. *J. Biol. Chem.* **278,** 42330–42339
41. Kenagy, R. D., Min, S. K., Clowes, A. W., and Sandy, J. D. (2009) Cell death-associated ADAMTS4 and versican degradation in vascular tissue. *J. Histochem. Cytochem.* **57,** 889–897
42. McCulloch, D. R., Nelson, C. M., Dixon, L. J., Silver, D. L., Wylie, J. D., Lindner, V., Sasaki, T., Cooley, M. A., Argraves, W. S., and Apte, S. S. (2009) ADAMTS metalloproteases generate active versican fragments that regulate interdigital web regression. *Dev. Cell.* **17,** 687–698
43. Enomoto, H., Nelson, C. M., Somerville, R. P., Mielke, K., Dixon, L. J., Powell, K., and Apte, S. S. (2010) Cooperation of two ADAMTS metalloproteases in closure of the mouse palate identifies a requirement for versican proteolysis in regulating palatal mesenchyme proliferation. *Development* **137,** 4029–4038
44. Hattori, N., Carrino, D. A., Lauer, M. E., Vasanji, A., Wylie, J. D., Nelson, C. M., and Apte, S. S. (2011) Pericellular versican regulates the fibroblast-myofibroblast transition A role for ADAMTS5 protease-mediated proteolysis. *J. Biol. Chem.* **286,** 34298–34310
45. Cattaruzza, S., Schiappacassi, M., Kimata, K., Colombatti, A., and Perris, R. (2004) The globular domains of PGM/versican modulate the proliferation-apoptosis equilibrium and invasive capabilities of tumor cells. *FASEB J.* **18,** 779–781